Limited-Area Fourier Spectral Models and Data Analysis Schemes: Windows, Fourier Extension, Davies Relaxation, and All That

JOHN P. BOYD

Department of Atmospheric, Oceanic, and Space Science, University of Michigan, Ann Arbor, Michigan

(Manuscript received 15 October 2004, in final form 3 January 2005)

ABSTRACT

Regional spectral models have previously periodized and blended limited-area data through ad hoc low-order schemes justified by intuition and empiricism. By using infinitely differentiable "window functions" or "bells" borrowed from wavelet theory, one can periodize with preservation of spectral accuracy. Similarly, it is shown through a mixture of theory and numerical examples that Davies relaxation for blending limited-area and global data in one-way nested forecasting can be performed using the same C^∞ bells as employed for the Fourier blending.

"The relative success of empirical methods . . . may be used as partial justification to allow us to make the daring approximation that the data on a limited area domain may be decomposed into a trend and a periodic perturbation, and to proceed with Fourier transformation of the latter." Laprise (2003, p. 775)

1. Introduction

For regional data analysis and weather forecasting, there are many technical advantages to tensor products of Fourier series in latitude and longitude. Consequently, there have been many spectral limited-area models (LAMs) as catalogued in Table 1. However, Laprise (2003) noted two serious deficiencies. First, "It shall be reiterated on purely mathematical grounds there is no justification for attempting to apply spectral transforms with global, periodic basis functions to nonperiodic fields defined on a limited-area domain." As shown below, this is not true, but he is quite right that spectral limited area models (SLAMs) have been derived heuristically through eighteenth-century physicomathematical intuition.

The second difficulty is that most SLAMs use rather crude procedures such that "the derivatives remain discontinuous" (Laprise 2003). This implies that if n is the total degree of a Fourier term and N is the truncation of the double Fourier series, then the coefficients fall only as $O(1/n^3)$ while the error decreases only as $O(1/N^2)$.

Mesinger (2000) (and others) assert that present-day limited-area models, whether spectral or not, are not greatly improved when the hydrodynamics is approximated with high-order methods; he suggests that to explain this woeful performance, "The forcing at individual model grid points done by physics packages of 'complete' models is the obvious prime candidate answer" (Mesinger 2000, p. 413). Still, using modern windowing/local Fourier basis technology, these derivative discontinuities can be banished: there is no reason to do badly what can be done well just as easily.

Laprise threw down a challenge: "The intent of this note is to stimulate reflections from readers who may be apt at suggesting a more satisfactory approach for scale decomposition of limited-area fields." The purpose of this article is to respond to his challenge and show that spectral limited-area modeling can be performed efficiently and accurately with preservation of high order.

2. Overview: Windows, extension, and relaxation

Regional spectral methods employ two technologies that will be analyzed in later sections. The first is Fourier extension: a nonperiodic function f must somehow be replaced by a modified function f^{ext}, which (i) agrees with f on the limited area and (ii) is spatially periodic on a larger domain so that the function can be expanded as

Corresponding author address: John P. Boyd, Dept. of Atmospheric, Oceanic, and Space Science, University of Michigan, 2455 Hayward Avenue, Ann Arbor, MI 48109-2143.
E-mail: jpboyd@umich.edu

TABLE 1. Spectral limited-area models and regional data analysis schemes.

Model	Country	Reference
LAM data analysis	United States	Errico (1985)
Japan Meteorological Agency (JMA) spectral-LAM	Japan	Tatsumi (1986); Segami et al. (1989); Sasaki et al. (1995); Hong et al. (1999)
Spectral-High Resolution Limited Area Model (HIRLAM)	Norway/Ireland	Haugen and Machenhauer(1993)
Arpege/Aire Limitée Adaptation Dynamique Développement International (ALADIN)	France	Bubnová et al. (1995)
Central Weather Bureau nested spectral	Taiwan	Juang et al. (2003)
Harmonic-sine spectral	United States	Chen and Kuo (1992); Chen et al. (1997)
Florida State University (FSU) nested regional spectral	United States	Cocke (1998); Cocke and LaRow (2000)
Spectral regional data analysis	Canada	Denis et al. (2002)
National Centers for Environmental Prediction (NCEP) spectral LAM	United States	Juang (1992); Juang and Kanamitsu (1994); Juang et al. (1997); Juang and Hong (2001)

a rapidly convergent Fourier series on the extended domain. The difference between the physical and Fourier domains is the "smoothing" or "extension" zone. The second technology is a method for smoothly blending high-resolution limited-area data with the lower-resolution global data that supplies boundary conditions for the LAM. We shall restrict attention to the most popular strategy, "Davies relaxation."

Spectral methods for nonperiodic problems fall into three broad categories

SLAM of the First Class is regional data analysis by means of tensor product Fourier series in latitude and longitude as in the work of Errico (1985), Chen and Kuo (1992), and Denis et al. (2002). Davies relaxation is unnecessary; the technical challenge is one of Fourier extension only. Because data are available in the extension zone, instead of being guessed or extrapolated, the problem is one of "Fourier Extension of the First Kind" in the language of Boyd (2002). It is only necessary to multiply f by a suitable "window" function to obtain f^{ext} as explained below.

SLAM of the Second Class is regional forecasting, as in the work of the others in the table. The need to blend the local forecast with data from the global model is a complication, but the merger strategy discussed later ("Davies relaxation") is likewise all a matter of windowing.

SLAM of the Third Class, which is a Fourier model that is *not* embedded in a global model, is not directly relevant to forecasting. However, theoretical studies of transition-to-turbulence and other flows have often found it advantageous to use a Fourier basis even for a nonperiodic problem as in Bertolotti et al. (1992), Högberg and Henningson (1998), Garbey (2000), Garbey and Tromeur-Dervout (1998, 2001), and Nordström et al. (1999). Regional spectral methods can *always* be justified, even for the most difficult case of SLAM of the Third Class where there is no global model or data.

3. Windows, bells, and imbrication

SLAM of the First Class defines the extended, periodized function f^{ext} using two key ideas. First, given a function $A(x)$ that goes to zero sufficiently fast as $|x| \to \infty$ so that the series converges, the function defined by

$$f^{\text{ext}}(x) = \sum_{m=-\infty}^{\infty} A(x - 2\Theta m) \tag{1}$$

is, by *construction*, *periodic* with period 2Θ. (See Table 2 for a list of the symbols used throughout this paper.) Such a series is called an "imbricate" series with $A(x)$ as the "pattern" function; it has been known for many decades that (i) every Fourier series can be written (nonuniquely) as an imbricate series and (ii) $A(x)$ is the Fourier transform of the Fourier coefficients of $f^{\text{ext}}(x)$ as explained in the review (Boyd 1989). For our purposes, though, the key idea is that by replicating an infinite number of copies of the "pattern" function, translating each copy so that one is centered every 2Θ on the entire real axis and summing, one can always obtain a periodic function even though the "pattern" is *not* periodic itself.

But how is one to create a "pattern" function that asymptotes to zero, and yet somehow preserves $f^{\text{ext}}(x) = f(x)$ on the physical domain? The answer is that the pattern function is created by multipying the (usually nonperiodic) function $f(x)$ by what is called a "window function" in signal processing or a "bell" in wavelet theory, $\mathcal{B}(x)$:

$$A(x) \equiv \mathcal{B}f. \tag{2}$$

Before cataloging the essential properties of a bell or window, it is first helpful to formally define the following.

TABLE 2. List of symbols.

Symbol	Meaning
$f(x)$	A nonperiodic function, such as the solution to a limited-area model
$f^{\text{ext}}(x)$	Periodic function that is the Fourier extension of $f(x)$
n	Fourier degree, i.e., a basis function is $\cos(nx)$ or $\sin(nx)$
$u_G(x, t)$	Solution of global model
$\tilde{u}_G(x, t)$	Equals u_G on $x \in [-\chi, \chi]$, identically zero elsewhere
$u_{\text{LAM}}(x, t)$	Solution of limited-area model
$\hat{u}_{LAM}(x, t)$	Limited-area solution before the Davies relaxation operation is applied
$\mathcal{B}$	Bell for Fourier extension
$\mathcal{E}$	Erf-like C^∞ function
$\mathbf{E}$	Fourier extension operator (in any number of spatial dimensions)
E_N	Error in approximating $f(x)$ by its Fourier series truncated after N cosines and N sines
$\mathcal{H}$	C^∞ smoothed step function
L	Map parameter, the internal parameter of the bell/window functions
N	Fourier truncation
$\mathcal{R}$	Bell for Davies relaxation
$\mathbf{T}_G$	Time evolution operator for global model (not including extension or Davies relaxation)
$\mathbf{T}_{\text{LAM}}$	Time evolution operator for limited-area model (not including extension or relaxation)
δ	Bound on $\delta_m(x, t)$
$\delta_m(x, t)$	Difference between global and limited-area solution, $\delta_m \equiv u_G - u_{LAM}$
υ	Viscosity coefficient
ρ	Davies relaxation is applied only for $\lvert x\rvert > \rho$ where $\rho < \chi$
τ	Time step
χ	Physical interval of limited-area model is $x \in [-\chi, \chi]$
Θ	The spatial period of Fourier-extended functions is 2Θ
Ξ	$\Xi \equiv \Theta - \chi$, half-width of the Fourier smoothing zones

Definition 1 (1D physical and extended intervals). The "physical" domain and "extended" domain are

$$x \in (-\chi, \chi) \text{ (Physical Interval)} \tag{3}$$

$$x \in (-\Theta, \Theta) \text{ (Extended Interval),} \tag{4}$$

where χ and Θ are positive constants and

$$\Theta > \chi. \tag{5}$$

The extended function f^{ext} is periodic with period 2Θ; that is, $f^{\text{ext}}(x + 2\Theta) = f^{\text{ext}}(x)\ \forall x$.

Definition 2 (C^∞ bell for Fourier extension. Here $\mathcal{B}(x)$ has the properties to be a satisfactory bell for Fourier extension if

1) $\mathcal{B} \equiv 1 \quad \forall x \in (-\chi, \chi)$;
2) $\mathcal{B}$ is infinitely differentiable everywhere on $x \in [-(2\Theta - \chi), (2\Theta - \chi)]$;
3) $\mathcal{B}$ is "infinitely flat" at $x = \pm\chi, \pm(2\Theta - \chi)$ in the sense that the bell and all its derivatives are zero at these points;
4) $\mathcal{B}$ is identically zero for $\lvert x\rvert > 2\Theta - \chi$.

The reason for the adjective "satisfactory" is that it is convenient but not necessary to impose additional properties on the bell as explained below.

Figure 1 illustrates a bell. Note that the "smoothing" zones do not end at the boundaries of the periodicity interval, $x \in (-\Theta, \Theta)$. The reason is that we use an "overlapped" extension (Boyd 2002), which is more efficient than the more obvious procedure of using a window that is identically zero everywhere outside the extended interval, $x \in (-\Theta, \Theta)$.

The easiest way to understand the "overlapped" extension is to draw the bell on a sheet of transparent acetate and then physically bend the sheet into a cylinder of circumference 2Θ. The edges of the sheet will overlap, and the graph of the bell will appear as in Fig. 2. However, the overlap is restricted to the overlapping left and right smoothing zones and does not extend into the physical interval where the bell is identically equal to one.

Overlapping the smoothing zones effectively *doubles* the width of the smoothing regions. This is helpful be-

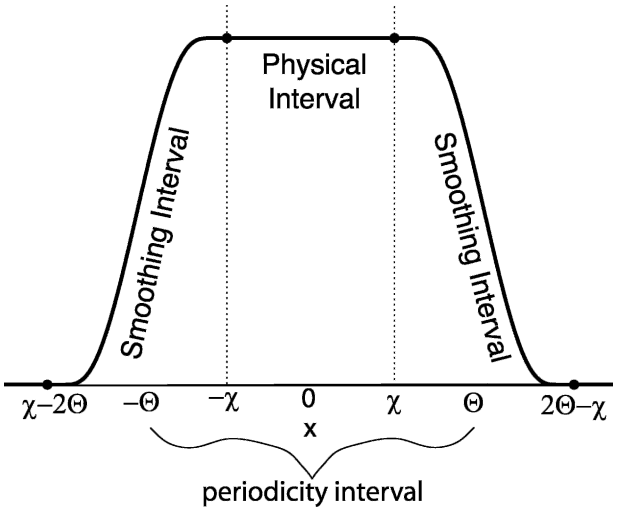

FIG. 1. Schematic of a C^∞ bell (window function). The physical interval, delineated by the vertical dotted lines, is $x \in (-\chi, \chi)$. Multiplication of f by the bell extends it to a function f^{ext}, which equals f on the physical interval and is periodic on the larger interval, $x \in (-\Theta, \Theta)$. The four black circles denote where the bell is "infinitely flat" in the sense that the bell and all its derivatives are zero at those points. The bell is identically one on the physical interval and identically zero for $\lvert x\rvert > 2\Theta - \chi$.

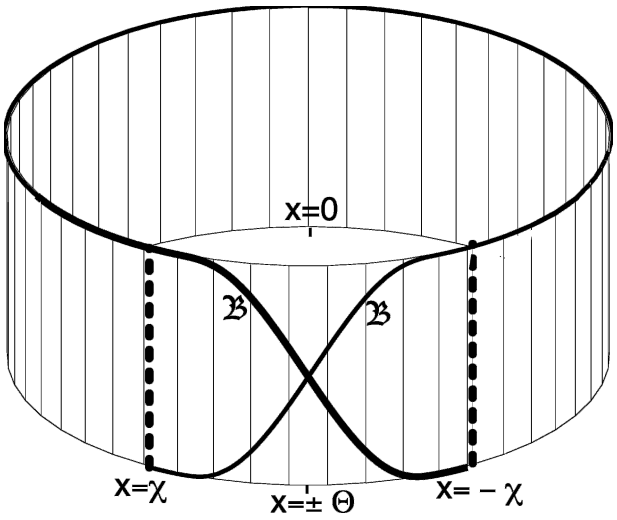

FIG. 2. By assuming that the extended, periodized function is periodic with period 2Θ, the interval is wrapped into a circle, and the graph of the bell (Fig. 1) becomes an overlapping curve on the surface of a cylinder. The point $x = \Theta$ is the same as $x = -\Theta$. The left and right smoothing zones on the interval become a single subinterval on the cylinder, bounded by the vertical dashed lines at $x = \pm\chi$. Note that $x = \chi$ is also, because of the periodicity, the point $x = -(2\Theta - \chi)$, and similarly $x = -\chi$ and $x = 2\Theta - \chi$ are the same point; x plays the role of a polar coordinate in a cylindrical coordinate system after the line graph has been wrapped into a cylinder. The bell $\mathcal{B}$ is identically equal to one everywhere on $x \in [-\chi, \chi]$.

cause the smoother the bell, the smoother the extended function, and the smoother $f^{\text{ext}}(x)$, the more rapidly its Fourier series converges.

One seemingly alarming feature of the overlapped extension is that it requires knowledge of $f(x)$, the (usually nonperiodic) function that is to be Fourier extended, on an interval that is larger than the periodicity domain, $x \in [-(2\Theta - \chi), (2\Theta - \chi)]$. We shall see in section 8, however, that the Fourier extension only has to be performed on data from the *global* model. Thus, the necessary data are always available if the global model is truly "global." The limited-area model (or data analysis) always employs a computational domain that is equal to the periodicity interval, $x \in (-\Theta, \Theta)$.

4. Convergence theorem for overlapped Fourier extension

Definition 3 (One-dimensional extension operator). Define **E** to be the operator that extends a function $f(x)$ to a periodic function f^{ext}:

$$f^{\text{ext}}(x) \equiv \mathbf{E} f(x) \equiv \sum_{m=-\infty}^{\infty} f(x - 2\Theta m) \times \mathcal{B}(x - 2\Theta m; \chi, \Theta), \quad \forall x. \tag{6}$$

Note that because the bell $\mathcal{B}$ has compact support (i.e., is identically zero for $|x| > 2\Theta - \chi$), only three terms actually contribute on the periodicity interval; that is,

$$f^{\text{ext}}(x) \equiv \mathbf{E} f(x) \equiv \sum_{m=-1}^{1} f(x - 2\Theta m) \times \mathcal{B}(x - 2\Theta m; \chi, \Theta), \quad x \in (-\Theta, \Theta). \tag{7}$$

Theorem 1 (Infinite-order Fourier convergence for bell-imbricate extensions). Suppose $f(x)$ is known and is analytic everywhere on $x \in [-(2\Theta - \chi), (2\Theta - \chi)]$. Let $\mathcal{B}$ denote a C^∞ bell as defined by definition 2 above. Extend f to a periodic function $f^{\text{ext}}(x)$ as in definition 3. Then,

1) the Fourier series for the extended function has "infinite order" convergence (Gottlieb and Orszag 1977; Boyd 2001) in the sense that its cosine and sine coefficients a_n, b_n satisfy the bounds

$$|a_n|, |b_n| \le \text{constant } n^{-k} \tag{8}$$

for arbitrarily large order k;

2) $$\left| f(x) - \sum_{n=0}^{N} a_n \cos[n(\pi/\Theta)x] + \sum_{n=1}^{N} a_n \sin[n(\pi/\Theta)x] \right| \le \frac{p}{N^k} \forall x \in (-\chi, \chi) \tag{9}$$

for some constant p (that may depend on k but not N) for arbitrarily large order k.

Proof: Because the bell $\mathcal{B}$ is infinitely differentiable for all x and is identically zero for $|x| > (2\Theta - \chi)$, the product of $\mathcal{B}$ with $f(x)$ is infinitely differentiable for all real x. This allows us to integrate by parts the Fourier coefficient integrals as many times as we please. The coefficients of the complex-exponential form of a Fourier series of period 2Θ are

$$c_n \equiv \frac{1}{2\Theta} \int_{-\Theta}^{\Theta} f^{\text{ext}}(x) \exp[-in(\pi/\Theta)x]\, dx, \tag{10}$$

where the cosine and sine coefficients are $a_n = 2\,\Re(c_n)$ and $b_n = -2\,\Im(c_n)$. After k integrations by parts, repeatedly integrating the exponential and differentiating $f(x)$,

$$c_n = \frac{1}{2\Theta} \sum_{j=0}^{k-1} (-1)^{j+1} \left(\frac{i\Theta}{n\pi}\right)^{j+1} [f^{\text{ext},j}(\Theta) - f^{\text{ext},j}(-\Theta)] + \frac{1}{2\Theta} \left(-\frac{i\Theta}{n\pi}\right)^k \int_{-\Theta}^{\Theta} \frac{d^k f^{\text{ext}}}{dx^k}(x) \exp[-in(\pi/\Theta)x]\, dx. \tag{11}$$

Since f^{ext} is the sum of an infinite number of identical copies of the "pattern" function $f(x)\ \mathcal{B}(x)$ [see Eq. (6)], it must be periodic. Since f^{ext} and its derivatives are the same at both $x = \Theta$ and $x = -\Theta$ because of the periodicity, all the boundary terms in (11) resulting from integration by parts are zero to all orders.

The integral in (11) can be bounded by a constant independent of degree n, namely,

$$\left|\int_{-\Theta}^{\Theta} f^{\text{ext},k}(x)\exp[-in(\pi/\Theta)x]\,dx\right| \le 2\Theta \max_{x\in(-\Theta,\Theta)}|f^{\text{ext},k}(x)|. \tag{12}$$

It follows that Fourier coefficients must be bounded by a constant times n^{-k} after k integrations by parts. Since k is arbitrary, the first proposition is proved.

Given that the coefficients are falling faster than any finite power of k, the second proposition follows immediately from theorem 9 plus (2.99) of Boyd (2001).

5. Explicit choice of bells and ramps

A vast number of functions are C^∞ bells as defined above. It is convenient to construct a large family of windows in terms of a smoothed approximation to the step function. Such a function is usually called a "ramp" in wavelet theory. It is convenient to express the ramp as

$$\mathcal{H}(x) \equiv (1/2)[1 + \mathcal{E}(x)], \tag{13}$$

where $\mathcal{E}$ is a function that resembles the error function with the property that $\mathcal{E} \equiv \text{sign}\,(x)$ for $|x| \ge 1$. The bell is identically equal to one in the "physical interval" and then is equal to the (scaled and translated) ramp in the left smoothing region and to a ramp with a negative argument on the right flank:

$$\mathcal{B}(x;\chi,\Theta) \equiv \begin{cases} \mathcal{H}\left(\dfrac{x+\Theta}{\Theta-\chi}\right), & x\in(-2\Theta+\chi,-\chi) \\ 1, & x\in(-\chi,\chi) \\ \mathcal{H}\left(-\dfrac{x-\Theta}{\Theta-\chi}\right), & x\in(\chi,2\Theta-\chi) \\ 0, & |x|>2\Theta-\chi. \end{cases} \tag{14}$$

Theorem 2 (Properties of bell and ramp). If the erf-like function $\mathcal{E}$ is antisymmetric with respect to x = 0—that is, $\mathcal{E}(-x) = -\mathcal{E}(x)$ for all x—then

1) $\mathcal{H}(x) + \mathcal{H}(-x) = 1, \quad x \in (-\infty,\infty);$ (15)

2) The bell $\mathcal{B}$ is a "partition-of-unity"; that is,

$$\sum_{m=-\infty}^{\infty} \mathcal{B}(x-2\Theta m) = 1, \quad x\in(-\infty,\infty); \tag{16}$$

3) If $f(x)$ is a periodic function with period 2Θ,

$$f^{\text{ext}}(x) = f(x) \quad x\in(-\infty,\infty). \tag{17}$$

Proof: The first proposition is proved by adding $\mathcal{H}(-x)$ to $\mathcal{H}-x)$ and then invoking the antisymmetry of $\mathcal{E}$ to replace $\mathcal{E}(-x)$ by $-\mathcal{E}(x)$, which causes both the factors of $\mathcal{E}$ to cancel. The second proposition follows by observing that in a given smoothing zone, only two copies of the bell are nonzero: for a given arbitrary integer k,

$$\begin{aligned} U &\equiv \sum_{m=-\infty}^{\infty} \mathcal{B}(x+2\Theta m) \\ &= \mathcal{B}(x-2k\Theta) + \mathcal{B}[x-2(k+1)\Theta], \\ &x\in[2k\Theta+\chi,(2k+2)\Theta-\chi]. \end{aligned} \tag{18}$$

Substituting in the definition of the bell gives

$$\begin{aligned} U &= \mathcal{H}\left[-\frac{x-(2k+1)\Theta}{\Theta-\chi}\right] + \mathcal{H}\left[\frac{x-(2k+1)\Theta}{\Theta-\chi}\right], \\ &x\in[2k\Theta+\chi,(2k+2)\Theta-\chi]. \end{aligned} \tag{19}$$

The first proposition then shows that $U = 1$ everywhere on the smoothing interval for all k. To prove the third proposition, observe that if $f(x)$ is periodic,

$$\begin{aligned} f^{\text{ext}}(x) &\equiv \sum_{m=-\infty}^{\infty} f(x-2\Theta m)\mathcal{B}(x-2\Theta m) \\ &= f(x)\sum_{m=-\infty}^{\infty} \mathcal{B}(x-2\Theta m). \end{aligned} \tag{20}$$

However, proposition 2 is that the infinite series multiplying $f(x)$ is one.

Only the properties of a C^∞ bell" catalogued in definition 2 are necessary for infinite order Fourier convergence of f^{ext}. However, the property of extending a periodic function without modification is desirable, too, because it implies that in this sense the extension distorts $f(x)$ as little as possible.

There are many possible choices for $\mathcal{E}$ that are antisymmetric and infinitely flat at the boundaries. Our preference, because the error function is free of singularities except at infinity, is

$$\mathcal{E}(x;L) = \begin{cases} -1, & x<-1 \\ \text{erf}\left(L\dfrac{x}{\sqrt{1-x^2}}\right), & x\in(-1,1). \\ 1, & x>1 \end{cases} \tag{21}$$

The parameter L is a scaling factor that specifies how rapidly the erf-like ramp and bell functions tend to their limits; appropriate values are discussed later.

Thanks to the $1/\sqrt{1-x^2}$, the argument of the error function varies from $-\infty$ to ∞ as x ranges from -1 to 1 so that $\mathcal{E}$ is infinitely flat (in the sense that all its derivatives vanish) at $x = \pm 1$. This allows the erf-like function, and by inheritance, the ramp and bell functions, to be infinitely differentiable for all real x (i.e., to belong to the function class C^∞).

The infinitely differentiable windows defined above are just as easy to apply as the various extension schemes used previously in spectral limited-area models. It is not at all necessary that, in Laprise's words, "the derivatives remain discontinuous."

6. Generalization to two space dimensions by tensor product

Definition 4 (Two-dimensional extension operator). To extend a function $f(x, y)$ from $(-\chi^x, \chi^x) \times (-\chi^y, \chi^y)$ so that it is doubly periodic with periods Θ^x in x and Θ^y in y, define $\mathbf{E}$ by

$$\mathbf{E}f \equiv \sum_{m=-\infty}^{\infty} \sum_{n=-\infty}^{\infty} f(x - 2\Theta^x m, y - 2\Theta^y n) \times \mathcal{B}(y - 2\Theta^y n)\mathcal{B}(x - 2\Theta^x m). \quad (22)$$

Because each bell is nonzero only on a finite interval, the sum indices can be reduced to ± 1 without altering the result. By construction, $\mathbf{E}f$ is periodic in both x and y with periods $2\Theta^x$ and $2\Theta^y$, respectively.

Theorem 3 (Infinite-order Fourier convergence: Two dimensions). Suppose $f(x, y)$ is known and is analytic everywhere on the rectangle $[-(2\Theta^x - \chi^x), (2\Theta^x - \chi^x)] \times [-(2\Theta^y - \chi^y), (2\Theta^y - \chi^y)]$. Let $f^{\text{ext}}(x, y) \equiv \mathbf{E}f$ where the extension operator $\mathbf{E}$ is defined by (22). Then,

1) the Fourier series for the extended function has "infinite order" convergence in the sense that

$$|a_{mn}, b_{mn}| \le \text{constant}(\sqrt{m^2 + n^2})^{-k} \quad (23)$$

for arbitrarily large order k;

2) $$\left| f(x) - \sum_{m=1N}^{N} \sum_{n=-N}^{N} c_{mn} \exp[im(\pi/\Theta^x)x + in(\pi/\Theta^y)y] \right| \le \frac{p}{N^k}, (-\chi^x, \chi^x) \times (-\chi^y, \chi^y) \quad (24)$$

for some constant p (that may depend on k) for arbitrarily large order k.

Proof: Identical in principle to the proof of theorem 1 except that the algebra is messier because of the extra index and coordinate.

7. Optimization and accuracy of Fourier extension

Since the behavior of f^{ext} in the smoothing region is of no interest, the relevant error is the error in the L_∞ norm on the *physical* interval:

$$E_N \equiv \max_{x \in [-\chi, \chi]} \left| f(x) - \sum_{n=0}^{N} a_n \cos(nx) + \sum_{n=1}^{N} b_n \sin(nx) \right|. \quad (25)$$

For a given function $f(x)$, the Fourier error E_N varies not only with the truncation N but also with the two remaining parameters. The first is the "scaling factor" L that appears in the definition of the bell via (21). The second is

$$\Xi \equiv \Theta - \chi, \quad (26)$$

which is the half-width of each of the two smoothing zones.

It is straightforward to compute the Fourier expansions for a given function and a given truncation N and various (Ξ, L) and plot the error as done for three different functions in Fig. 3. The optimum pair of (Ξ, L) (black circles) is different for each $f(x)$. However, some general tendencies may be noted.

First, the error is a flat plateau around its minimum. This implies that rather large deviations of the numerical parameters L and Ξ from their optimum values raise the error only slightly.

Second, when $f(x)$ is very smooth (upper left), the optimum Ξ is rather large. The reason is that when $f(x)$ is smoother than the bell $\mathcal{B}$, it is advantageous to use a rather wide extension zone (large Ξ). The larger the smoothing zone, the smoother is the bell. Thus, it is optimum to widen the extension zone until the smoothness of the very wide bell is increased to that of $f(x)$.

In contrast, the second and third examples have much more structure: the former has narrow boundary layers near $x = \pm 1$ while the latter is a trigonometric polynomial of very high degree. For these, it is best to use a much narrower region with $\Xi \approx 0.3$, that is, smoothing zones whose combined width is only a third of the width of the physical interval.

Third, the optimum internal parameter L of the bell varies with the functions, too, from three to six, depending on the example. In general, the rougher the function, the smaller is the best choice of L.

Fourth, it is possible to achieve very high accuracy—a maximum pointwise error of 10^{-6} or less—for

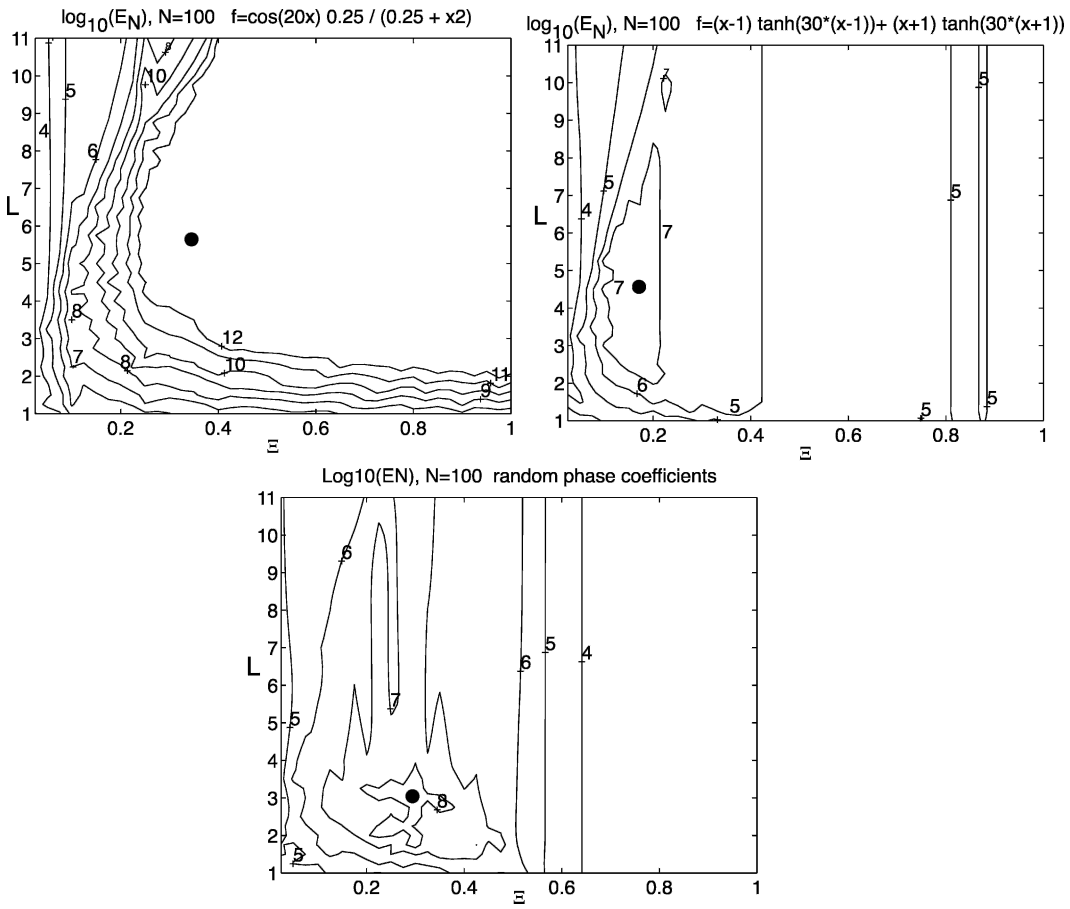

FIG. 3. Isolines of the negative of $\log_{10}$ of the L_∞ error on the physical interval, chosen to be $x \in (-1, 1)$, for three different functions $f(x)$, plotted vs the map parameter L of the bell (vertical axis) and vs the width of the smoothing zones, $\Xi \equiv \Theta - 1$, where the Fourier series is periodic on the extended interval $x \in (-1 - \Xi, 1 + \Xi)$. N = 100 cosines for these functions, which are all symmetric with respect to $x = 0$ (solely for convenience). The functions are (upper left) $f = \cos(20x)\ (1/4)/(1/4 + x^2)$, (upper right) $f = (x - 1)\tanh[30(x - 1)] + (x + 1)\tanh[30(x + 1)]$, and (bottom) the sum of a truncated Fourier cosine series of degree 200 with coefficients proportional to the inverse square of the degree, multiplied by a random number between -1 and 1. The contour labels denote powers-of-10; thus "7" denotes the contour line where $E_N = 10^{-7}$. The heavy black dots denote roughly the minimum error for each function.

a very wide range of (L, Ξ) for all of the examples. The third example was deliberately chosen to have a slowly decreasing Fourier spectrum to mimic the not very smooth power-law spectra of atmospheric flows. Even so, 100 cosines, or 200 terms of a general sine-and-cosine Fourier series, suffice for very high accuracy.

Weather forecasting, of course, is not so precise. Turbulent flows have power-law Fourier spectra instead of the much faster exponential decrease of amplitude with wavenumber k that is characteristic of Fourier approximations to analytic functions. Furthermore, geophysical models make no attempt to satisfy the "compatibility conditions" at the boundaries as explained in Boyd and Flyer (1999), Flyer and Swarztrauber (2002), and Flyer and Fornberg (2003a,b). In addition, $\Xi = 1/3$ gives a computational overhead of about a factor of 2 in two dimensions; modelers might choose to reduce this overhead even at the expense of a nonoptimum smoothing domain, especially since the error is not very sensitive to Ξ.

Still, there is no reason to do badly what can be done well. The numerical examples show that while regional forecasting and climate models have many ills, inaccurate Fourier extension need not be one of them.

8. Blending global and limited-area data

For simplicity, we shall restrict discussion to one-way nested models in which the global model is integrated independently of the regional model so that the cou-

pling is only global-to-LAM. Although two-way nested models are widely used, too, the simpler one-way nested codes will suffice to illustrate our major themes.

The simplest way to blend global with regional data is known variously as "Davies relaxation," "Newtonian damping," or "Rayleigh friction" and is a particular case of the more general strategy of "nudging" the limited-area model toward the global flow at the boundaries. This relaxation is sometimes implemented by adding a term to the time-dependent equations. For our experiments, we use a simpler implementation, which is to apply, at the end of each time step, the blending, with $\mathcal{R}(x)$ the "relaxation bell" defined by (29) below:

$$u_{\mathrm{LAM}}(t^n) = [1 - \mathcal{R}(x)]u_{\mathrm{global}}(t^n) + \mathcal{R}(x)\hat{u}_{\mathrm{LAM}}(t^n), \tag{27}$$

where $\hat{u}_{\mathrm{LAM}}(t^n)$ is the unblended LAM output at the nth time level t^n.

Global-to-local blending is closely related to extending a nonperiodic function to a periodic function. Indeed, one can use the same bell for both. The only difference is that the smoothing interval must be different.

It is a bad idea to use a Davies blending region that is narrower than the periodization window because the Davies factor will degrade the Fourier convergence of the periodic function u_{LAM} more than the periodization. From a theoretical point of view, the most sensible choice—and also the simplest—is to use extension and relaxation regions of *equal size*.

This is a little subtle because the extension zone in the overlapped extension is effectively *twice* the width Ξ of the subinterval $x \in (\chi, \Theta)$. Furthermore, theorems presented below show that Davies relaxation can be overlapped with Fourier smoothing. Thus, the zones for Davies relaxation can be taken as

$$|x| \in (\rho, \Theta), \quad \rho = \chi - (\Theta - \chi). \tag{28}$$

The interval $x \in (\rho, \chi)$, where there is Davies relaxation but no Fourier smoothing, is of the same width Ξ as the interval on which both Davies relaxation and Fourier windowing occurs, $x \in (\chi, \Theta)$.

The relaxation bell $\mathcal{R}$ is then, with $\chi = \rho + \Xi$ and $\Theta = \rho + 2\Xi$ for some positive, user-chosen Ξ,

$$\mathcal{R}(x; \rho, \Theta) \equiv \begin{cases} \mathcal{H}[(x + \chi)/(\Theta - \chi)], & x \in (-\Theta, -\rho) \\ 1, & x \in (-\rho, \rho). \\ \mathcal{H}[-(x - \chi)/(\Theta - \chi)], & x \in (\rho, \Theta) \end{cases} \tag{29}$$

Figure 4 is similar to Fig. 2 except that the Davies smoothing interval (bounded by short dashed lines at $x = \pm\rho$) and the Davies window $\mathcal{R}$ (dotted) have been added.

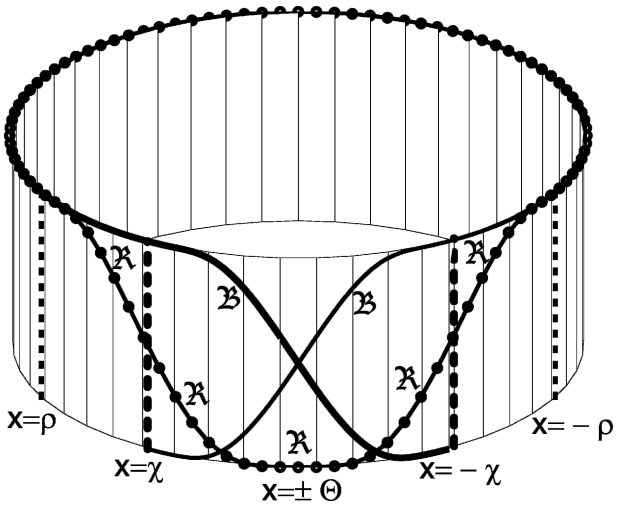

FIG. 4. By assuming that the extended, periodized function is periodic with period 2Θ, the interval is wrapped into a circle, and the line graphs of the periodization bell and Davies bell becomes curves on the surface of a cylinder as shown. The point $x = \Theta$ is the same as $x = -\Theta$. The thinner dashed lines mark the points $x = \pm\rho$, which are the boundaries of the physical interval. The Davies window is dotted and labeled by $\mathcal{R}$. There are two periodization windows shown by a thick solid line and a somewhat thinner line, both labeled by $\mathcal{B}$. All the windows are identically one everywhere on the physical interval, which is the part of the cylinder away from the viewer, bounded by the thin vertical lines.

9. Relaxation and extension errors: A theorem

A fundamental question is, how much error is introduced by Davies relaxation? A partial answer is given by the following theorem.

Theorem 4. Suppose that a coupled global–limited-area model is integrated by the following procedure where $\mathbf{T}_G$ and $\mathbf{T}_{\mathrm{LAM}}$ are the nonlinear time evolution operator of the models for t $\in [0, \tau]$ where τ is the time step and $u_G(x, t)$ and $u_{\mathrm{LAM}}(x, t)$ are the global and limited-area solutions:

1) $\hat{u}_{\mathrm{LAM}}(x, \tau) = \mathbf{T}_{\mathrm{LAM}}\mathbf{E}u_G(x, 0)$
2) $u_{\mathrm{LAM}}(x, \tau) = (1 - \mathcal{R})\mathbf{E}u_G(x, \tau) + \mathcal{R}\hat{u}_{\mathrm{LAM}}(x, \tau)$.

Define, for an arbitrary function $\upsilon(x)$

$$\delta_m(x, t; \upsilon) \equiv \mathbf{T}_G\upsilon - \mathbf{T}_{\mathrm{LAM}}\upsilon. \tag{30}$$

Then if

$$|\mathbf{T}_{\mathrm{LAM}}\mathbf{E}u_G(x, 0) - \mathbf{T}_{\mathrm{LAM}}u_G(x, 0)| < \epsilon \quad \forall x \in (-\rho, \rho) \tag{31}$$

and, for all $\upsilon(x)$ such that $|\max \upsilon| \le \max |u_G|$ on $x \in [-\rho, \rho]$,

$$|\delta_m(x, t; \upsilon)| \le \delta \tag{32}$$

for small $\delta > 0$, then

$$|u_{\mathrm{LAM}}(x, \tau) - u_G(x, \tau)| < \epsilon + \delta \quad \forall x \in (-\rho, \rho). \tag{33}$$

In words, if the exact solution is insensitive to alterations in $u_G(x, t)$ for the region $|x| > \chi$ where the Fourier extension modifies the global solution—insensitivity meaning the difference is smaller than some small parameter ϵ—then the LAM/global coupling with Davies relaxation will not produce errors larger than $\epsilon + \delta$ on the physical domain where δ is the bound on differences produced by the different resolution and other properties of the limited-area evolution operator $\mathbf{T}_{\mathrm{LAM}}$ versus $\mathbf{T}_G$.

Proof: The solution to the limited-area model is

$$\hat{u}_{\mathrm{LAM}}(x, \tau) = \mathbf{T}_{\mathrm{LAM}}\mathbf{E}u_G(x, 0) \quad \forall x. \tag{34}$$

However, $\mathbf{E}$ is the identity operator on the interval $x \in (-\chi, \chi)$. The extension operator modifies the initial condition and induces an error $\epsilon_{\mathrm{LAM}}(x, \tau)$, but Eq. (31) requires that this error is bounded by ϵ. It follows that on the physical interval, the extension operator disappears and

$$\hat{u}_{\mathrm{LAM}}(x, \tau) = \mathbf{T}_{\mathrm{LAM}}u_G(x, 0) + \epsilon_{\mathrm{LAM}}(x, \tau) \quad \forall x \in (-\rho, \rho). \tag{35}$$

The global solution will evolve, too, but with a different time evolution operator:

$$u_G(x, \tau) = \mathbf{T}_G u_G(x, 0) = \mathbf{T}_{\mathrm{LAM}}u_G(x, 0) + \delta_m(x, \tau; u_G) \tag{36}$$

because of Eq. (32). Davies relaxation gives

$$\begin{aligned} u_{\mathrm{LAM}}(x, \tau) &= (1 - \mathcal{R})u_G(x, \tau) + \mathcal{R}[\mathbf{T}_{\mathrm{LAM}}u_G(x, 0) \\ &\quad + \epsilon_{\mathrm{LAM}}(x, \tau)] \\ &= (1 - \mathcal{R})u_G(x, \tau) + \mathcal{R}[\mathbf{T}_G u_G(x, 0) \\ &\quad - \delta_m(x, \tau; u_G) + \epsilon_{\mathrm{LAM}}(x, \tau)] \\ &= (1 - \mathcal{R})u_G(x, \tau) + \mathcal{R}[u_G(x, \tau) \\ &\quad - \delta_m(x, \tau; u_G) + \epsilon_{\mathrm{LAM}}(x, \tau)] \\ &= u_G(x, \tau) + \mathcal{R}[-\delta_m(x, \tau; u_G) \\ &\quad + \epsilon_{\mathrm{LAM}}(x, \tau)], \quad x \in (-\rho, \rho), \end{aligned} \tag{37}$$

where we have used $\mathbf{E}u_G = u_G$ on $x \in (-\chi, \chi)$. Recalling from the assumptions that $\delta_m(x, \tau, u_G)$ and ϵ_{LAM} are bounded by δ and ϵ proves the theorem.

The theorem is all well and good, but somewhat abstract. The function $\delta_m(x, t)$ is not really an error, but merely the difference between the global model and the higher-resolution limited-area model. Thus, ε is the only error that arises from windowing and Davies relaxation.

The first important point is that ε is caused solely by the Fourier extension algorithm and is *independent* of the Davies relaxation $\mathcal{R}$; Davies relaxation is constructed so that it does not induce errors.

The second point is that the extension error ε depends on how *localized* is the dynamics embodied in the evolution operator $\mathbf{T}$. Fourier windowing modifies $u_G(x, t)$ only for $|x| > \chi$; the physical interval—the only domain where the limited-area solution will be graphed, analyzed, and trusted—is the *smaller* interval $x \in (-\rho, \rho)$. The extension will introduce errors only to the extent that the modifications to the global solution for $|x| > \chi$ are able to propagate to within the physical interval within a *single time step*.

For example, suppose that the physics is restricted to linear, nondispersive advection at a phase speed c. Fourier extension will be error-free provided that

$$c\tau < \chi - \rho, \tag{38}$$

that is, provided the waves cannot propagate as far as the distance $\chi - \rho$ in a single time step of length τ. Now the Courant–Friedrichs–Lewy (CFL) time step limit for an explicit time-marching scheme is $c\tau < h$ where h is the spatial grid size. Since the buffer zones for Davies relaxation and Fourier extension are roughly 10 h (in order of magnitude), it follows that the extension and Davies relaxation produce no errors unless the time step is an order of magnitude larger than the CFL limit. This is possible only with implict time marching—but it is well known that implicit schemes gain their stability by slowing down wave speeds so that the CFL limit is satisfied (Boyd 2001). Thus, nondispersive advection never introduces errors in practice.

Pure diffusion is another instructive example; that is, suppose that the model problem is

$$u_t = \nu u_{xx}, \tag{39}$$

then

$$\begin{aligned} u(x, \tau) &= \mathbf{T}u(x, 0) \\ &= \frac{1}{\sqrt{4\pi\nu\tau}} \int_{-\infty}^{\infty} u(y, 0) \exp\left[-\frac{(y - x)^2}{4\nu\tau} \right] dy. \end{aligned} \tag{40}$$

In contrast to advection, diffusion is *not local*; that is, changes in the initial condition at any point on the real axis will alter the solution *everywhere*. However, the influence of a given point falls exponentially fast. Define

$$\mathbf{T}\mathbf{E}u(x, 0) - \mathbf{T}u(x, 0) \equiv \epsilon_{\mathrm{LAM}}(x, \tau). \tag{41}$$

Now on the interval $x \in (-\chi, \chi)$, only a single copy of the pattern function is nonzero and $\mathcal{B} \equiv 1$ everywhere on this interval. It follows without approximation that

$$\epsilon_{\mathrm{LAM}} = \frac{1}{\sqrt{4\nu\pi\tau}} \int_{-\infty}^{-\chi} \left[\sum_{m=-\infty}^{\infty} \mathcal{B}(y - 2m\Theta, 0) \times u(y - 2m\Theta) - u(y, 0)] \exp\left[-\frac{(y-x)^2}{4\nu\tau} \right] + \frac{1}{\sqrt{4\nu\pi\tau}} \int_{\chi}^{\infty} \left[\sum_{m=-\infty}^{\infty} \mathcal{B}(y - 2m\Theta, 0) \times u(y - 2m\Theta) - u(y, 0)] \exp\left[-\frac{(y-x)^2}{4\nu\tau} \right] \right].$$

To obtain a bound, we can replace the expressions in brackets by their upper bound, which is $\max |u(x, 0)|$. This gives

$$|\epsilon_{\mathrm{LAM}}| \le \frac{\max|u(x,0)|}{\sqrt{4\nu\pi\tau}} \left| \int_{-\infty}^{-\chi} \exp\left[-\frac{(y-x)^2}{4\nu\tau} \right] \right| + \frac{\max|u(x,0)|}{\sqrt{4\nu\pi\tau}} \left| \int_{\chi}^{\infty} \exp\left[-\frac{(y-x)^2}{4\nu\tau} \right] \right|.$$

Since the two integrands decay exponentially as $|x| \to 0$,

$$|\epsilon_{\mathrm{LAM}}| \le \frac{\max|u(x,0)|}{\sqrt{\pi\nu\tau}} \exp\left[-\frac{(\chi-\rho)^2}{4\nu\tau} \right] \quad \forall x \in [-\rho, \rho]. \tag{42}$$

If the time step τ is sufficiently small to satisfy the CFL criterion, $\nu\tau < h^2$, and $\chi - \rho \approx 10\,h$, then the exponential in the bound will be $\exp(-25) \approx 10^{-11}$, which is ridiculously small compared to the errors of typical forecasts.

One can do similar estimates for dispersive waves and other physical processes, but the punch line is always the same: unless the process can leap the interval $\chi - \rho$, which is typically 10 grid spacings h, in a single time step, the Fourier extension does not contaminate the solution on the physical interval $x \in (-\rho, \rho)$.

10. Numerical illustration

Burgers' equation,

$$u_t + uu_x = \nu u_{xx}, \tag{43}$$

has the family of exact solutions

$$u(x,t) = c - B \tanh\left\{ B\left(\frac{x - ct - \phi}{2\nu} \right) \right\} \quad \text{[Taylor shock]} \tag{44}$$

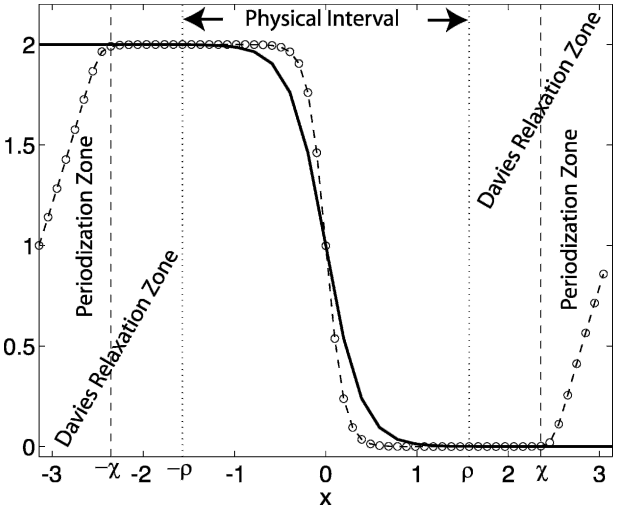

FIG. 5. Propagation of a Taylor shock into a limited-area model for Burgers' equation. The global solution at $t = (3/2)\pi$ is the solid curve; the limited-area solution $u_{\mathrm{LAM}}[x, (3/2)\pi]$ is the dashed curve with circles. The physical interval is $x \in ([-\pi/2, \pi/2)$, i.e., $\rho = \pi/2$. Davies relaxation is applied on $|x| \in (\pi/2, \pi)$. An overlapping Fourier windowing is applied for $|x| > 3\pi/4 = \chi$. The limited-area model used 64 grid points. The (extended) limited-area solution is periodic with period 2π.

where (B, c, ϕ) are constants. Choosing somewhat arbitrarily the parameters $c = 1$, $B = 1$, and $\phi = -(3/2)\pi$, we applied a SLAM embedded in a global model that was also Fourier, but with a domain 8 times larger.

The SLAM initial condition is the windowed "Taylor shock":

$$u_{\mathrm{LAM}}(x,0) = \left[1 - \tanh\left(\frac{x - (3/2)\pi}{2\nu} \right) \right] \mathcal{B}(x; \chi, \Theta, L) + \left[1 - \tanh\left(\frac{x + 2\Theta - (3/2)\pi}{2\nu} \right) \right] \times \mathcal{B}(x + 2\Theta; \chi, \Theta, L) + \left[1 - \tanh\left(\frac{x - 2\Theta - (3/2)\pi}{2\nu} \right) \right] \times \mathcal{B}(x - 2\Theta; \chi, \Theta, L). \tag{45}$$

To mimic common numerical practice, the viscosity coefficient ν was set equal to the (nondimensional) spatial grid spacing h in both the LAM and global models. Because of the higher resolution of the limited-area model (where $h = \pi/32$ versus a grid spacing of $\pi/16$ for the global model), the LAM viscosity was only half as large as for the global model. As illustrated in Fig. 5, the LAM gracefully evolved to a Taylor shock whose frontal zone was only half as wide as that of the traveling shock in the global model—the higher resolution of the LAM really did allow for a sharper shock.

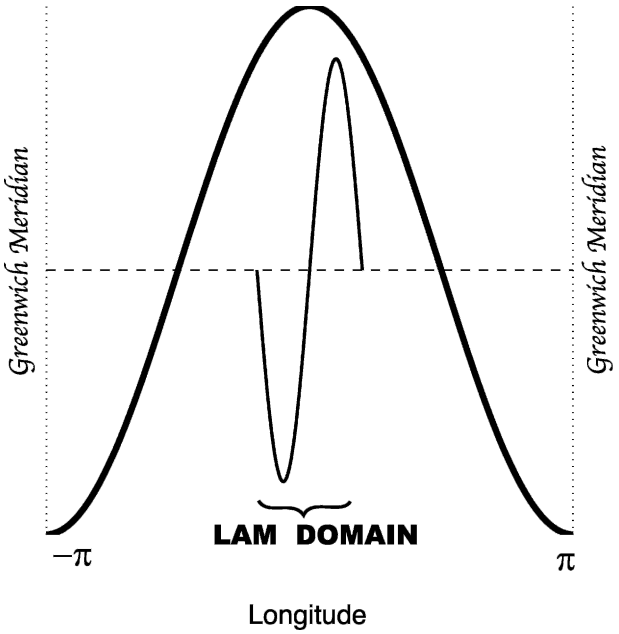

FIG. 6. Schematic of a circle of latitude. If λ is longitude, then the lowest Fourier component on the sphere is cos(λ) (thick solid curve) [and similarly sin(λ); not shown]. The longest Fourier components of a series defined on say, one-fifth of the globe, are cos(5λ) and sin(5λ) (thin curve).

11. Ultralong waves and spectral nudging

The literature of limited-area models, whether spectral or finite difference is full of worry about ultralong waves. Planetary wavenumber 1 (Fig. 6) and other long waves do not fit within the limited-area domain. If the longitudinal width of the LAM is one-fifth of the globe, for example, then the longest wave that will fit is $\exp(i5\lambda)$ where λ is longitude. For data analysis, one should therefore take the common-sense approach of computing the ultralong waves from global data and only the short waves from the higher-resolution regional data.

But how are ultralong waves approximated, periodized, and Davies-relaxed? Theorem 1 shows that all such worries are misplaced: the theorem applies to the ultralong waves as it does to all other scales of motion. Figure 7 is a visual confirmation, displaying the Fourier coefficients for an ultralong wave (left) and also for a short wave (right). (It seems puzzling that an ultralong wave can "have any sensible projection on a limited-area domain" in the words of a reviewer, but the crucial point is that the long wave is multiplied by a *window* and *periodized* by imbricate series; the Fourier-extended ultralong wave does have a "sensible projection.") For both functions, the Fourier coefficients on the limited domain fall exponentially fast. For numerical purposes, no special tricks are needed.

The first physics worry is that waves are reflected by the jump in resolution between the coarse grid of the global model and the finer grid of the LAM. The difference between the global and limited-area solutions, dubbed $\delta_m(x, y, t)$ in theorem 4, is a mixture of error and improvement. The narrower front of the LAM solution is a *difference* from the coarse-and-more-viscous global model, but also an *improvement* that justifies the LAM. Unfortunately, a jump in resolution is the same as any other jump in index of refraction, causing spurious partial reflections (Vichnevetsky and Scheidegger 1991). These grid-induced reflections, alas, are pure error. The theorem shows that extension and relaxation with C^∞ bells will neither amplify nor damp these errors.

However, the waves that reflect are the *short waves*, that is, those that are not resolved or only marginally resolved by the global model. Well-resolved waves have almost the same speed—very close to the exact phase speed—on either side of a jump in grid spacing. Thus, no special treatment for reflected waves is needed either.

The second physics worry is that the global and limited-area models will diverge over time because of exponential growth of the differences due to the differences in resolution and other parameters: the usual loss-of-predictability problem first pointed out by Lorenz more than forty years ago. This is an issue unrelated to Fourier extension or Davies relaxation, but is unfortunately intrinsic to nonlinear chaotic dynamics.

A common strategy to reduce such physics difficulties is "spectral nudging," which means that the ultralong wave is constrained to mimic the global model, independent of the limited-area dynamics (Miguez-Macho et al. 2004, and references therein). Except perhaps to deal with the chaos-driven exponential-in-time growth of differences between the global and limited-area models, spectral nudging, and indeed any special numerical treatment of the ultralong waves, is therefore *unnecessary* for one-way nested models if Fourier extension and Davies relaxation are done with spectral accuracy (theorem 4). The apparent success of spectral nudging for one-way nesting is at least partly an artifact of very bad procedures for windowing and blending.

12. Summary and conclusions

Laprise's "daring approximation" of using a Fourier series to approximate the nonperiodic flow of a limited-area model can be made rigorous by using C^∞ window functions. Regional forecasting also requires Davies relaxation or some similar procedure to blend the global data into the higher-resolution LAM. This, too, can be

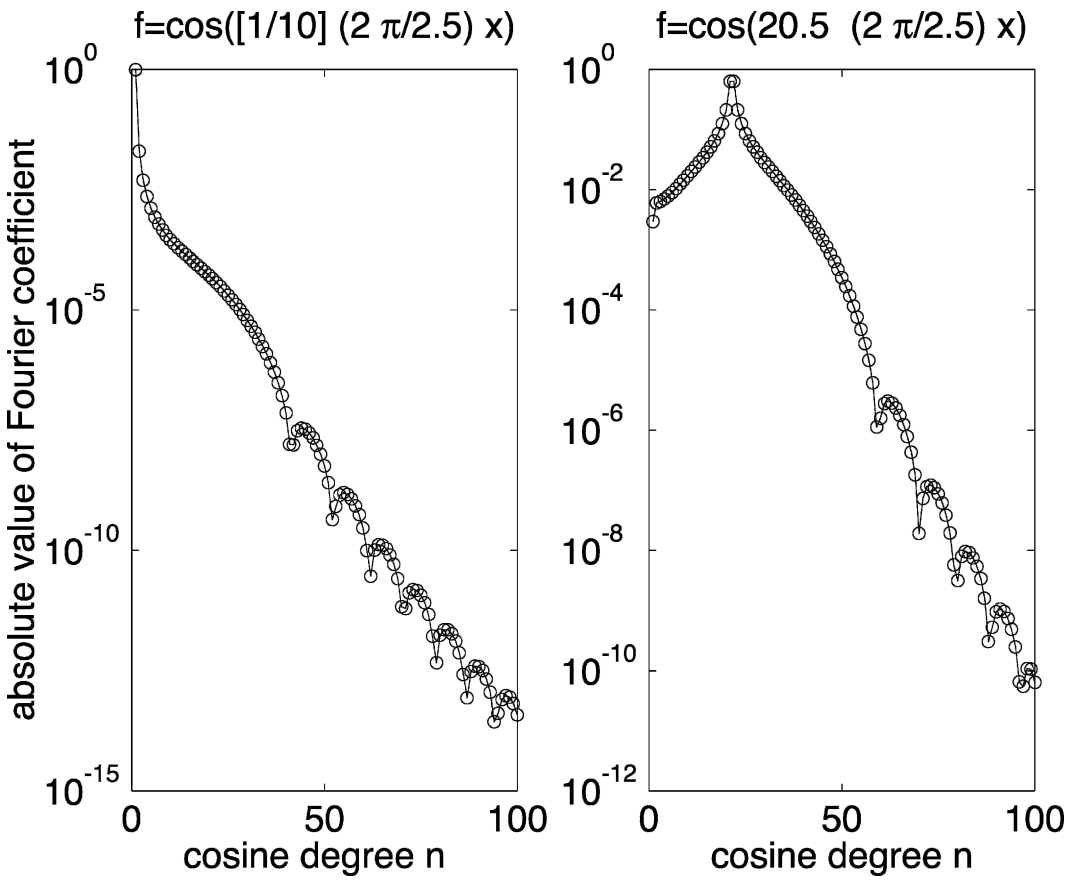

FIG. 7. Fourier expansion of two windowed and extended functions on $x \in (1.25, 1.25)$: (left) $f(x)$ is a cosine function whose spatial period is 10 times the width of the extended interval, and (right) f is a cosine whose wavenumber is halfway between the twentieth and twenty-first cosine basis functions for the extended domain. For both graphs, $L = 5$ and $\Xi = 1/4$; the curves would be qualitatively similar for different L and Ξ where L is internal parameter of the bell function and Ξ is the width of the smoothing zones. The horizontal axis plots n where the Fourier functions are $[\cos(nx), \sin(nx)]$.

done using the same window functions (but with different widths) as the Fourier extension. Both procedures can be implemented so that the windowing errors fall as *exponential* functions of the number of degrees of freedom N.

Of course real limited-area models have many sources of error, and full "spectral accuracy" for turbulent weather is unattainable. The theorem of section 9 shows that errors are small for an interval of one time step, but cannot restrict the exponential growth of differences between limited-area and global models that are generic to chaotic nonlinear dynamics. Furthermore, the *physics* of the interaction of limited-area and global models, and of models of different resolution, is complex and poorly understood.

These qualifications, however, are no justification for ad hoc, low order blending procedures. The *approximation theory* issues in limited-area modeling can be solved even though some of the physics issues remain intractable. Fourier blending and Davies relaxation can be applied with both rigor and accuracy.

Acknowledgments. This work was supported by NSF Grant OCE9986368. I thank René Laprise and an anonymous reviewer for unusually detailed comments that greatly improved this work.

REFERENCES

Bertolotti, F. P., T. Herbert, and P. R. Spalart, 1992: Linear and nonlinear stability of the Blasius boundary layer. *J. Fluid Mech.,* **242,** 441–474.

Boyd, J. P., 1989: New directions in solitons and nonlinear periodic waves: Polyenoidal waves, imbricated solitons, weakly non-local solitary waves and numerical boundry value algorithms. *Advances in Applied Mechanics,* T.-Y. Wu and J. W. Hutchinson, Eds., Vol. 29, Academic Press, 1–82.

——, 2001: *Chebyshev and Fourier Spectral Methods.* 2d ed. Dover, 665 pp.

——, 2002: A comparison of numerical algorithms for Fourier

extension of the First, Second, and Third kinds. *J. Comput. Phys.,* **178,** 118–160.

——, and N. Flyer, 1999: Compatibility conditions for time-dependent partial differential equations and the rate of convergence of Chebyshev and Fourier spectral methods. *Comput. Methods Appl. Mech. Eng.,* **175,** 281–309.

Bubnová, R., G. Hello, P. Bénard, and J. Geleyn, 1995: Integration of the fully elastic equations cast in the hydrostatic pressure terrain-following coordinate in the framework of the ARPEGE/Aladin NWP system. *Mon. Wea. Rev.,* **123,** 515–535.

Chen, Q.-S., and Y.-H. Kuo, 1992: A harmonic-sine series expansion and its application to partitioning and reconstruction problems in a limited area. *Mon. Wea. Rev.,* **120,** 91–112.

——, L. Bai, and D. H. Bromwich, 1997: A harmonic-Fourier spectral limited-area model with an external wind lateral boundary condition. *Mon. Wea. Rev.,* **125,** 143–167.

Cocke, S., 1998: Case study of Erin using the FSU nested regional spectral model. *Mon. Wea. Rev.,* **126,** 1337–1346.

——, and T. E. LaRow, 2000: Seasonal predictions using a regional spectral model embedded within a coupled ocean–atmosphere model. *Mon. Wea. Rev.,* **128,** 689–708.

Denis, B., J. Côté, and R. Laprise, 2002: Spectral decomposition of two-dimensional atmospheric fields on limited-area domains using the Discrete Cosine Transform (DCT). *Mon. Wea. Rev.,* **130,** 1812–1829.

Errico, R. M., 1985: Spectra computed from a limited area grid. *Mon. Wea. Rev.,* **113,** 1554–1562.

Flyer, N., and P. N. Swarztrauber, 2002: The convergence of spectral and finite difference methods for initial-boundary value problems. *SIAM J. Sci. Comput.,* **23,** 1731–1751.

——, and B. Fornberg, 2003a: Accurate numerical resolution of transients in initial-boundary value problems for the heat equation. *J. Comput. Phys.,* **184,** 526–539.

——, and ——, 2003b: On the nature of initial-boundary value solutions for dispersive equations. *J. Comput. Phys.,* **64,** 546–564.

Garbey, M., 2000: On some applications of the superposition principle with Fourier basis. *SIAM J. Sci. Comput.,* **22,** 1087–1116.

——, and D. Tromeur-Dervout, 1998: A new parallel solver for the nonperiodic incompressible Navier–Stokes equations with a Fourier method: Application to frontal polymerization. *J. Comput. Phys.,* **145,** 316–331.

——, and ——, 2001: Parallel algorithms with local Fourier basis. *J. Comput. Phys.,* **173,** 575–599.

Gottlieb, D., and S. A. Orszag, 1977: *Numerical Analysis of Spectral Methods.* SIAM, 200 pp.

Haugen, J. E., and B. Machenhauer, 1993: A spectral limited-area model formulation with time-dependent boundary conditions applied to the shallow-water equations. *Mon. Wea. Rev.,* **121,** 2618–2630.

Högberg, M., and D. S. Henningson, 1998: Secondary instability of cross-flow vortices in Falkner–Skan–Cooke boundary layers. *J. Fluid Mech.,* **368,** 339–357.

Hong, S., H. H. Juang, and D. Lee, 1999: Evaluation of a regional spectral model for the East Asian monsoon case studies for July 1987 and 1988. *J. Meteor. Soc. Japan,* **77,** 1–20.

Juang, H. H., 1992: A spectral fully compressible nonhydrostatic mesoscale model in hydrostatic sigma coordinates: Formulation and preliminary results. *Meteor. Atmos. Phys.,* **50,** 75–88.

——, and M. Kanamitsu, 1994: The NMC nested regional spectral model. *Mon. Wea. Rev.,* **122,** 3–26.

Juang, H. M. H., and S. Y. Hong, 2001: Sensitivity of the NCEP regional spectral model to domain size and nesting strategy. *Mon. Wea. Rev.,* **129,** 2904–2922.

——, ——, and M. Kanamitsu, 1997: The NCEP regional model: An update. *Bull. Amer. Meteor. Soc.,* **78,** 2125–2143.

——, C. H. Shiao, and M. D. Cheng, 2003: The Taiwan Central Weather Bureau regional spectral model for seasonal prediction: Multiparallel implementation and preliminary results. *Mon. Wea. Rev.,* **131,** 1832–1847.

Laprise, R., 2003: Resolved scales and nonlinear interactions in limited-area models. *J. Atmos. Sci.,* **60,** 768–779.

Mesinger, F., 2000: Numerical methods: The Arakawa approach, horizontal grid and limited-area modeling. *General Circulation Model Development: Past, Present and Future,* D. Randall, Ed., International Geophysical Series, Vol. 70, Academic Press, 373–419.

Miguez-Macho, G., G. L. Stenchikov, and A. Robock, 2004: Spectral nudging to eliminate the effects of domain position and geometry in regional climate model simulations. *J. Geophys. Res.,* **109,** D13104, doi:10.1029/2003JD004495.

Nordström, J., N. Nordin, and D. Henningson, 1999: The fringe region technique and the Fourier method used in the direct numerical simulation of spatially evolving viscous flows. *SIAM J. Sci. Comput.,* **20,** 1365–1393.

Sasaki, H., H. Kida, T. Koide, and M. Chiba, 1995: The performance of long-term integrations of a limited area model with the spectral boundary coupling method. *J. Meteor. Soc. Japan,* **73,** 165–181.

Segami, A., K. Khara, H. Nakamura, M. Ueno, I. Takano, and Y. Tatsumi, 1989: Operational mesoscale weather prediction with Japan spectral model. *J. Meteor. Soc. Japan,* **67,** 907–923.

Tatsumi, Y., 1986: A spectral limited-area model with time-dependent lateral boundary conditions and its application to a multi-level primitive equation model. *J. Meteor. Soc. Japan,* **64,** 637–663.

Vichnevetsky, R., and T. Scheidegger, 1991: The nonlocal nature of internal reflection in computational fluid dynamics with spectral methods. *Appl. Numer. Math.,* **8,** 533–539.